IARJSET
ISSN (Online) 2393-8021
ISSN (Print) 2394-1588
International Advanced Research Journal in Science, Engineering and Technology
ISO 3297:2007 Certified
Vol. 3, Issue 12, December 2016

The Effective Role of P_2O_5 on Structural and Morphological Properties of SiO_2-CaO-P_2O_5 Dried Gels

P. Kiran[1], N. K. Udayashankar[1] and H. D. Shashikala[1]

Department of Physics, National Institute of Technology, Karnataka Surathkal, India[1]

Abstract: 58SiO_2-(38-x) CaO-(x+4) P_2O_5 dried gels (x=0, 5, 10 and 15mol%) dried gel samples were synthesized at drying temperature 130°C by conventional sol-gel method. For synthesis used precursors are Tetraethyl ortho-silicate (TEOS), Tri ethyle phosphate (TEP), Calcium nitrate tetra hydrate for SiO_2, CaO and P_2O_5 compositions. Structural properties were studied for synthesized dried gels using X-Ray diffraction (XRD), Fourier Transform Infrared (FTIR), Raman spectroscopic analysis and Field Emission Scanning Electronic Microscopy (FESEM) with Energy dispersive X-ray diffraction (EDX) analysis. XRD pattern indicated that all dried gel samples have amorphous nature. FTIR spectroscopic analysis show that more P_2O_5 content leads to increasing degree of polymerization. Raman spectroscopic analysis indicates that increasing P_2O_5 content decreases the intensity of orthophosphate structures i.e., increasing P_2O_5 decreases orthophosphate structural units. Using FESEM average pore sizes of synthesized dried gels are calculated as 143.51, 149.54, 173.25, 182.81 micrometers for corresponding P_2O_5 mol% of 4, 9, 14 and 19 respectively. From all these observations increasing P_2O_5 decreases number of orthophosphate units and increases degree polymerization, it leads to increasing pore size on dried gel surface.

Keywords: Sol-gel; P_2O_5 composition; Calcium oxide; Pore size.

1. INTRODUCTION

Sol-gel derived calcium phosphosilicate glasses were created historical wonder in biomedical field because of their saving applications. These glasses can form bone and regenerate tissues in physiological environment like simulated body fluid (SBF) solution. The bio active nature of theses glasses are mainly depends on both strength of implanted materials like silica glass matrix, and hydroxy carbonated apatite (HCA) layer formation in SBF solution [1].

Depending on drying and stabilization temperature, sol-gel derived glass shows variation in porosity. The porous nature of these glasses leads to the formation of calcium phosphate layer in SBF solution. Porosity observed after drying at lower temperature in sol-gel derived glasses is advantages compares with melts quenched glasses. This is because the formation of HCA layer in SBF solution mainly depends on movement of calcium and phosphate ions through the silica matrix. Melt derived glass matrix has higher density than that of porous sol-gel derived glasses which results the movement of ions. The oxide glasses like SiO_2, Ge_2O, B_2O_3 and P_2O_5 can form three dimensional random net-works by themselves [2].

Only silicate glass can use like a single component glass. Increasing the composition of alkali or alkaline oxides decreases the number of bridging oxygens and increases the number of non-bridging oxygens by maintaining the total charge neutrality in between alkali or alkaline cation and oxygen anion. Q^4 structure has SiO_4^{-4} tetrahedra with four bridging oxygens, Q^3 has the SiO_4^{-3} tetrahedra with three bridging oxygens and one non bridging oxygen, Q^2 has the SiO_4^{-2} tetrahedra with two bridging oxygens and two non bridging oxygens while Q^1 has the SiO_4^{-1} tetrahedra with one bridging oxygen, three non bridging oxygens and Q^0 has the SiO_4 tetrahedra with four non bridging oxygens. While adding alkali or alkaline oxides to SiO_2 the tetrahedra changes from Q^4 to Q^3, $Q^3$to Q^2, Q^2 to Q^1 and Q^1 to Q^0 [3-6]. The internal network connectivity between network formers and network modifiers changes the densities of glasses. Lower densities and higher drying temperatures increase pore densities [7].

Due to their properties of higher refractive index, thermal shock resistance, optical transparency in both the UV and visible regions and high chemical durability, silica glasses can be used in the semiconductor industry as a crucible for the formation of silicon, a mask blank for photolithography. Main drawback of this material is higher temperature required for preparation of glasses (2000 °C) in melt quenching method. [1].

SiO_4^{-4} and PO_4^{-3} cannot form complete solution in the glass, because of the difference in bond strength of SiO_4^{-4} and PO_4^{-3}. Also SiO_4^{-4} and PO_4^{-3} groups may be capable of co-polymerization and for low P_2O_5, P^{+5} may substitute for Si^{+4}. For higher amount of P_2O_5, Si-O-P link can form in the glass. The Si-O-P bond may lead to the bending vibration of SiO_6 octahedral rather than silicon tetrahedra [8, 9]. For the preparation of silicate glasses sol-gel technique is the best technique since it enhances its bioactivity through formation of pores [10, 11]. And also

IARJSET
ISSN (Online) 2393-8021
ISSN (Print) 2394-1588
International Advanced Research Journal in Science, Engineering and Technology
ISO 3297:2007 Certified
Vol. 3, Issue 12, December 2016

sol-gel process is low temperature process with low cost [12]. During the last decade silica-based bioactive glasses have supplied successful solutions to different bone defects and soft tissue treatments [13,14]. The high biocompatibility and the positive biological effects of silicate glasses encourage their usage as bio ceramics [3, 8, 12, 15-21]. Ohtsuki et all (1992) observed that the formation of apatite layer on P_2O_5 contained CaO-SiO_2 glasses is greater than P_2O_5 free CaO-SiO_2 glass [22, 23]. The FTIR spectroscopy and Raman spectroscopic studies can give clear explanations of assigned bands in the glass structure [24, 25]. Particularly concentration of the non bridging oxygens in silica matrix can be easily estimated by Raman spectroscopy [26-28].

In present study sol-gel derived 58SiO_2-(38-x) CaO-(x+4) P_2O_5 dried gels where x=0, 5, 10, 15 have been synthesized. The effective role of P_2O_5 on Structural and surface morphological properties of prepared samples are discussed.

2. MATERIALS AND METHODS

2.1. Synthesis

58SiO_2-(38-x) CaO-(x+4) P_2O_5 [x= 0, 5, 10 and 15 mol %] dried gels were synthesized by conventional sol-gel process and samples were named as CPS1, CPS2, CPS3 and CPS4 respectively as shown in **Table 1**. The preparation of the present glasses were achieved from the precursors such as tetraethylorthosilicate [$Si(OC_2H_5)_4$], triethylphosphate (TEP) [$(C_2H_5O)_3$ PO], calcium nitrate tetra hydrate [Ca $(NO_3)_2$ $4H_2O$] 2N Nitric acid (HNO_3) and double distilled water. Water and HNO_3 were selected as [(mol of H_2O)/(mol of TEOS+ mol of TEP) =10] and [(mol of HNO_3)/(mol of TEOS+ mol of TEP) =0.05] respectively.

In order to synthesize the glass sample, tetraethylorthosilicate (TEOS) was mixed with water and nitric acid and stirred for one hour. At an interval of one hour TEP and calcium nitrate were added subsequently and stirred well. The prepared sols were poured into teflon beakers, sealed with aluminum wrappers and kept inside hot air oven at 60°C for three days of aging, subsequently the aged gels were dried at 130 °C for 4 hours. The dried gels were ground, made into powder.

2.2. Characterizations

The structural properties of calcium phosphosilicate dried gels have been studied by X-ray diffraction technique, using Powder X-ray Diffractometer (PXRD) (JOEL, JDX-8P). The chemical characterization was performed by FTIR method (SHIMADZU spectrometer). For IR analysis, the first 1 mg of material scarped calcium phosphosilicate gels were carefully mixed with 300 mg of KBr (infrared grade) and palletized.

Then the prepared pellets were analyzed in the range between 400 to 3000 cm^{-1} at a scan rate of 25 scan/min with the resolution of 4 cm^{-1}. Room temperature Raman spectroscopy was performed using a LABRAM-HR800 Laser Raman Spectrometer with 514 nm laser radiation. To avoid laser heating of the samples, the incident power was kept at a low value of 1.99 mW. Field emission scanning electron microscopy (FESEM, Carl Zeiss Ultra 55 model) of the centrifuged samples was used for the morphological analysis of the prepared powder samples. Sigma Scan Pro software was used to determine the average pore size of powder samples of CPS dried gels.

3. RESULTS AND DISCUSSION

The XRD analysis results of CPS gel samples are shown in **Fig. 1(a)** Those samples almost take amorphous sates indicative of internal disorder and it is worth mentioning that CPS gels don't show any crystalline states [29]. As shown in FTIR spectra [**Fig.1(b)],** for CPS dried gels different intensity signal occurs at around 462-478 cm^{-1} related to bending modes of Si-O-Si (**Table 1**).

The adsorption peaks at 941-972 cm^{-1} are very strong, assigned to the Si-O-Si asymmetric stretching vibrations. Si-O-Si symmetric stretching modes are observed around the wave number of 825 cm^{-1}. Si-O-NBO bands are assigned at 915-933 cm^{-1} wave number region. PO_4^{3-} stretching modes of vibrations are also observed at 1195-1342 cm^{-1} wave number regions. CPS1 gel has more pronounced stretching modes of PO_4^3 tetrahedra and SCP4 glass has the least. Increasing of P_2O_5 content shifted the PO_4^{3-} stretching vibrations to higher wave number side. Si-O-P (as s), CO_3^{2-} (bend) modes are observed at the wave number region 1033-1056 cm^{-1}, 1438-1442 cm^{-1} respectively. Water molecules (H_2O), OH-groups are also observed at the wave number regions of 1620-1697 cm^{-1}, 2345-2360 cm^{-1} respectively[30].Raman spectra show [**Fig.1(c)**] PO_4^{3-} orthophosphate stretching modes (Q^0(P)) as s) are assigned at the wave number regions 1050-1051 cm^{-1}. Q^0(P) intensities have increased from CPS1 dried del to CPS4 dried gel. It indicates that $Q^0(P)^-$ intensities are decreased with increasing P_2O_5 content for CPS dried gels [29].

Using FESEM images average pore sizes are calculated as 143.51, 149.54, 173.25, 182.81 micro meters for CPS1, CPS2, CPS3, and CPS4 dried gels as shown in **Fig.2**. It indicates that increasing P_2O_5 content increases average pore size of materials. EDX analysis indicates that presented elements are in the gel structure are Si, Ca, P and O [30]. Porosity influence effects not only internal structure but also glass surface. Porosity represents the accommodations of water molecules in glass matrix. At drying and stabilization processes large amount of shrinkage leads to fracture on glass surface. The excessive shrinkage is caused by a capillary forces, induced by liquid evaporation in micro pores which has given as $P=2\gamma\cos\theta/D$, Where P, γ, ɵ, D are capillary force, liquid surface tension, liquid contact angle and micro pore diameters respectively [2]. This reason causes the increasing surface pore size from nano meter to micrometer range.

IARJSET
ISSN (Online) 2393-8021
ISSN (Print) 2394-1588
International Advanced Research Journal in Science, Engineering and Technology
ISO 3297:2007 Certified
Vol. 3, Issue 12, December 2016

4. CONCLUSIONS

SiO_2-P_2O_5-CaO dried gel samples were synthesized at drying temperature 130°C by conventional sol-gel method. Structural properties were studied for synthesized dried gels using X-Ray diffraction (XRD), Fourier Transform Infrared (FTIR), Raman spectroscopic analysis and Field Emission Scanning Electronic Microscopy (FESEM) with Energy dispersive X-ray diffraction (EDX) analysis. XRD pattern indicated that all dried gel samples have shown amorphous nature. FTIR spectroscopic analysis show increasing P_2O_5 content increases prominence of PO_4^{3-} asymmetric stretching mode.

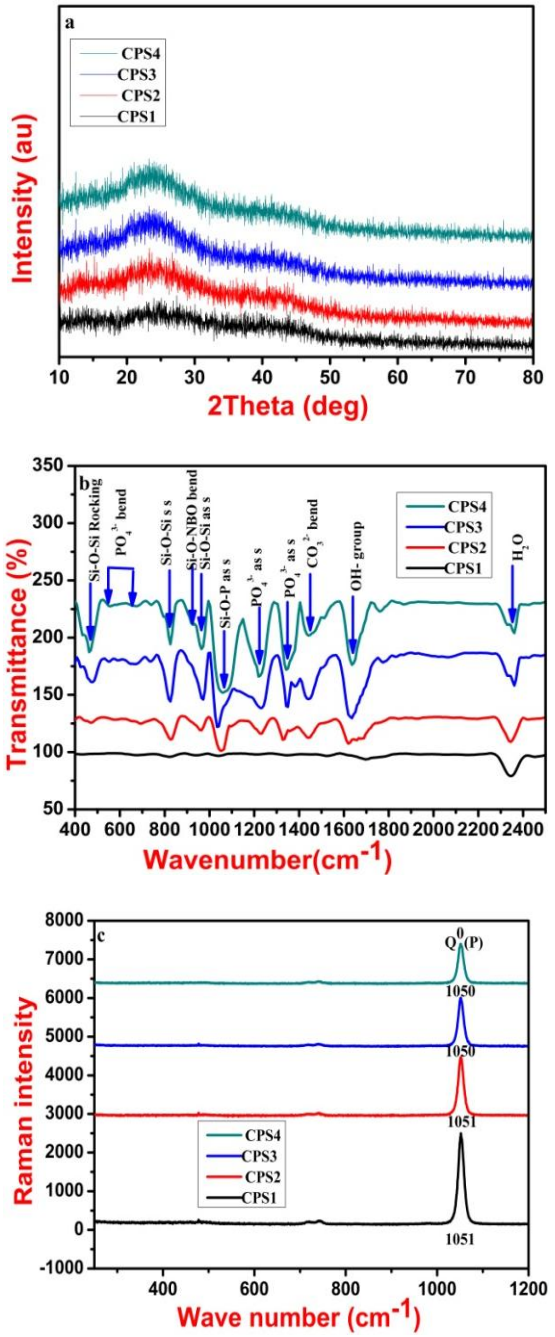

Fig. 1(a) XRD pattern **(b)**, **(c)** FTIR, Raman spectra of CPS dried gels

Raman spectroscopic analysis indicates that increasing P_2O_5 content decreases the intensity of orthophosphate structures i.e., increasing P_2O_5 decreases orthophosphate structural units. Because increasing P_2O_5 content increases 3-dimensional network connectivity in polymerization process. Increasing P_2O_5 with decreasing CaO increases local structural defects. These defects act as hosts for water molecules. So, increasing P_2O_5 content increases the defect volumes. Increasing volume may causes for more water molecule accommodations.

In drying process water molecules can evaporate through the surface of dried gel with capillary forces, this leads to formation of pores with different sizes on glass surface. The pore size depends on size of evaporated water molecules through gel surface. The evaporated water molecule size may increase with increasing P_2O_5 content in CPS dried gels. It leads to increasing average pore size on glass surface with increasing P_2O_5 content in CPS dried gels. Hence it can say that increasing P_2O_5 content increases surface pore size of synthesized calcium phospho silicate dried gels.

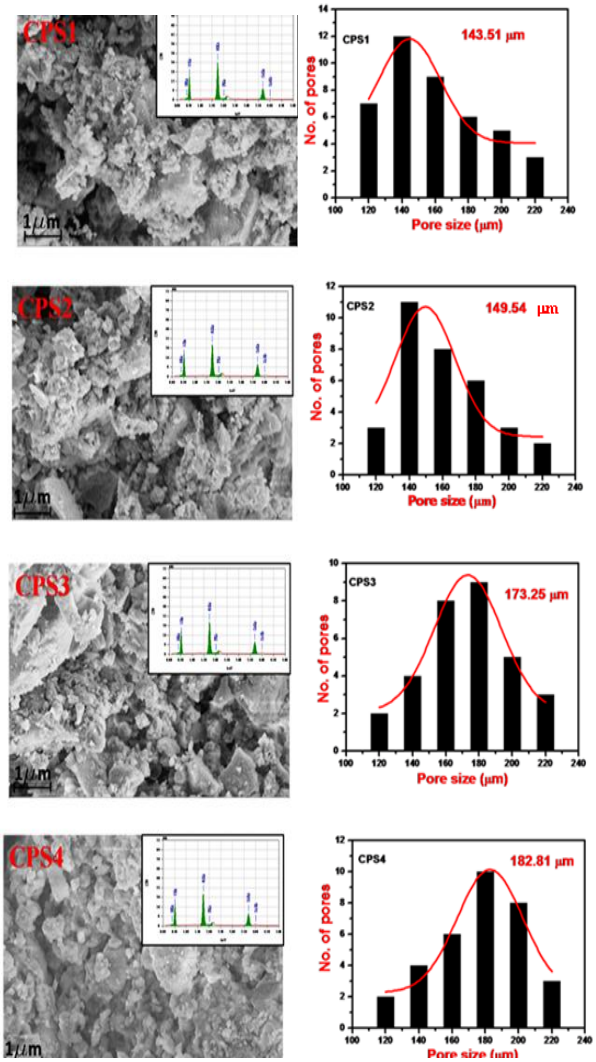

Fig. 2 FESEM/EDX images of CPS dried gels with corresponding pore size distribution

IARJSET
ISSN (Online) 2393-8021
ISSN (Print) 2394-1588
International Advanced Research Journal in Science, Engineering and Technology
ISO 3297:2007 Certified
Vol. 3, Issue 12, December 2016

Table 1 FTIR band assignments CPS gels Infrared transition band in cm^{-1}

CPS1 (cm^{-1})	CPS2 (cm^{-1})	CPS3 (cm^{-1})	CPS4 (cm^{-1})	Assigned bands
478	478	478	462	Si-O-Si rocking
625-685	569-650	556-659	565-680	PO_4^{-3} bending
825	825	825	825	Si-O-Si symmetric stretching (s s)
898	915	918	933	Si-O-NBO asymmetric stretching(as s)
941	964	972	964	Si-O-Si asymmetric stretching (as s)
1041	1049	1033	1056	Si-O-P asymmetric stretching (as s)
1195, 1342	1226, 1326	1234, 1350	1218, 1342	PO_4^{-3} asymmetric stretching (as s)
-	1438	1442	1442	CO_3^{2-} bending
1697	1620	1615	1635	OH group
2345	2345	2360	2360	H_2O

ACKNOWLEDGEMENTS

Authors gratefully acknowledge to National Institute of Technology Karnataka, Surathkal, for providing research facilities and financial support.

REFERENCES

[1] L.L. Hench, Genetic design of bioactive glass, J. Eur. Ceram. Soc., 29 (2009) 1257-1265.
[2] J. E. Shelby, Introduction to glass science and technology, Second Edition 2005.
[3] M. R. Majhi, P. Ram and S.P. Singh, Studies on preparation and characterizations of CaO-Na_2O-SiO_2-P_2O_5 bio glass ceramics substituted with Li_2O, K_2O, ZnO, MgO, and B_2O_3 International Journal of Scientific &Engineering Research., 9 (2011) 2229.
[4] J. Ma,C. Z. Chen, D. Z. Wang and J. Z. Shi, Textural and structural studies of sol–gel derived SiO_2–CaO–P_2O_5–MgO glasses by substitution of MgO for CaO, Mater. Sci. Eng., C, 30 (2010) 886-890.
[5] L. Courtheoux, J. Lao, J. Nedelec and E. Jallot, Controlled Bioactivity in Zn-doped sol-gel derived SiO_2-CaO bioactive glasses, J. Phys. Chem. C., 35 (2008) 13663-13667.
[6] S. Rajendra Kumar, G. P. Kothiyal and A. Srinivasan, In vitro evaluation of bioactivity of CaO–SiO_2–P_2O_5–Na_2O–Fe_2O_3 glasses, Appl. Surf. Sci., 255 (2009) 6827-6831.
[7] J. Ma, C. Z. Chen, D. G. Wang,Y. Jiao and J. Z. Shi, Effect of magnesia on the degradability and bioactivity of sol-gel derived SiO_2-CaO-MgO-P_2O_5 system glasses, Colloids Surf., B: Biointerfaces., 81 (2010) 87-95.
[8] Md. Rafiqul Ahsan and M. Golam Mortuza, Infrared spectra of xCaO-(1-x-z) SiO_2-zP_2O_5 glasses, J. Non-Cryst. Solids., 351 (2005) 2333-2340.
[9] H. R. Ahamd Mooghari, A. Nemati, Y. B. Eftekhari, Z. Hamnabard, The effects of SiO_2 and K_2O on glass forming ability and structure of CaO-TiO_2-P_2O_5 glass system, Ceram. Int., 38 (2012) 3281-3290.
[10] B. Lei, X. Chen, Y. Wang, N. Zhao and C. Du, Synthesis and bioactive properties of macroporous nanoscale SiO_2–CaO–P_2O_5 bioactive glass, J. Non-Cryst. Solids 355 (2009) 2678-2681.
[11] L. Gerhardt and R. Boccaccini, Bioactive Glass and Glass-Ceramic Scaffolds for Bone Tissue Engineering, Materials. 3 (2010) 3867-3910.
[12] A. Daniel and V. María, Sol–gel silica-based biomaterials and bone tissue regeneration, Acta Biomaterialia., 6 (2010) 2874-2888.
[13] O.Nieves, A. Martın Antonio, J. Salinas, J. Turnaya, M. Vallet-Reg and M.A. Lizar. Bioactive sol–gel glasses with and without a hydroxyl carbonate apatite layer as substrates for osteoblast cell adhesion and proliferation, Biomater, 24 (2003) 3383-3393.
[14] R. K. Singh and A. Srinivasan, Bioactivity of SiO_2–CaO–P_2O_5–Na_2O glasses containing zinc–iron oxide, Appl. Surf.h Sci. 256 (2010) 1725-1730.
[15] M. Mami, A. Lucas-Giorat, H. Oudadesse, R. Dorbaz-Sridi, F. Mezahi and E. Ditrich, Investigationof thesurface reactivity of sol-gel derived glass in the ternary system SiO_2-CaO-P_2O_5Appl. Surf. Sci. 254 (2008) 7386-7393.
[16] F. Talos, A. Vulpoi,A. Ponton,A. Simon, D. Dudea and S. Bran, Orianted growth of apatite-like crystals at the interface between a silicate nano composite and simulated body fluid, Digest Journal of Nano materials and Bio structures (2013) 219-225.
[17] W. Lui, K. Li, C. Lu, L. G. Teoh, W. H. Wu and Y. C. Shen. Synthesis and Characterization of Mesoporous $SiO_2CaOP_2O_5$ Bioactive Glass by Sol-Gel Process, Metall. Trans. 54 (2013) 791-795.
[18] R. L. Siqueira, O. Peitl Oscar and E. D. Zanotto Edgar, Gel-derived SiO_2–CaO–Na_2O–P_2O_5 bioactive powders: Synthesis and in vitro bioactivity, Mater. Sci. Eng., C.31 (2011) 983-991.
[19] C. Shu, Z. Wenjuan, G. Xu, Z. Wei, J. Wei and W. Dongmei, Dissolution behavior and bioactivity study of glass ceramic scaffolds in the system of CaO–P_2O_5–Na_2O–ZnO prepared by sol–gel technique, Mater. Sci. Eng C., 30 (2005) 105-111.
[20] A. Balamurugan, G. Balossier, D. Laurent-Maquin, S. Pina, A.H.S Rebelo, J. Faure and J. M. F. Ferreira, An in vitro biological and anti-bacterial study on a sol–gel derived silver-incorporated bioglass system, Dent. Mater., 24 (2008) 1343-1351.
[21] S. Asgharnia Shirin and P. Alizadeh, Synthesis and characterization of SiO_2–CaO–P_2O_5–MgO based bioactive glass and glass-ceramic nano fibres by electro spinning, Materials Letters. 101 (2013) 107-110.
[22] S. Ni, R. Du and S. Ni, The Influence of Na and Ti on the In Vitro Degradation and Bioactivity in 58S Sol-Gel Bioactive Glass, Advances in Materials Science and Engineering 2012, Article ID 730810.
[23] A. Ramila, M. Vallet-Regm, A. Ramila and M. Vallet-Regm, Static and dynamic in vitro study of a sol-gel glass bioactivity, Biomater., 22 2001) 2301-2306.
[24] H. Aguiar, J. Serra, P. González and B. Leon, Structural study of sol–gel silicate glasses by IR and Raman spectroscopies, J. Non-Cryst. Solids., 355 (2009) 475-480.
[25] P. Gonzalez, J. Serra, S. Liste, S. Chiussi, B. Leon and M. Perez-Amor, Raman spectroscopic study of bioactive silica based glasses, J. Non-Cryst. Solids. 320 (2003) 92-99.
[26] J. Wong, Vibrational spectra of vapour deposited binary phosphosilicate glasses, J. Non-Cryst. Solids., 20 (1976) 83-100. S
[27] B. O. Mysen, D. Virgo and C. M. Scarfe, Relations between the anionic structure and viscosity of silicate melts a Raman spectroscopic study American Mineralogis., 65 (1980) 690-710.
[28] W. L. Konijnendijk and J. M. Stevels, Raman scattering measurements of Silicate glasses and compounds, J. Non-Cryst. Solids., 21 (1976) 447-453.
[29] Y. Sun, Z. Zhang, L. Liu and X. Wang,FTIR, Raman and NMR investigation of CaO-SiO_2-P_2O_5 and CaO-SiO_2-TiO_2-P_2O_5 glasses, J. Non-Cryst. Solids., 420 (2015) 26-33.
[30] X. Yang, L. Zhang, X Chen, X.Sun, G.Yang, X. Guo, H. Yang, C GaO and Z. Gou, Incorporation of B_2O_3 in CaO-SiO_2-P_2O_5 bio active glass system for improving strength of low temperature co-fired porous glass ceramics J. Non-Cryst. Solids., 358 (2012) 1171-1179.